

## New approximate solutions to Duffing's Equation

G. Höhler and I. Sabba-Stefanescu  
Institut für Theoretische Kernphysik  
University of Karlsruhe, West Germany

---

We have investigated approximations to Duffing's equation  $\ddot{x} + 2\Delta\dot{x} + x^3 = \Gamma \cos t$  and numerical solutions for large values of  $\Gamma$  and a wide range of  $\Delta$ , including the limits  $\Gamma \rightarrow \infty$ ,  $\Delta = \Gamma^\alpha$ . The results are also valid for the equivalent equation  $\ddot{x} + 2\Omega\Delta\dot{x} + x^3 = \cos \Omega t$  with  $\Omega = 1/\Gamma^{1/\alpha}$ , which describes the motion of a particle in a slowly time-dependent potential  $V(x,t) = x^4/4 - x \cos \Omega t$ .

$x(t)$  is represented as a superposition of a slowly varying background  $x_r(t)$ , which approximately corresponds to the location of the minimum of the moving potential and  $u(t) := x(t) - x_r(t)$ , which is a rapid oscillation for small  $\Delta$  and large  $\Gamma$ .  $x_r(t)$  is defined as the solution of the relaxation equation  $2\Delta\dot{x}_r + x_r^3 = \Gamma \cos t$ .

A linearized version of the equation for  $u(t)$  is sufficient in a large domain of the  $\Gamma, \Delta$ -plane, including the above mentioned limits for  $\alpha > 0$ . For small values of  $\Delta$  and large  $\Gamma$ , the harmonic solutions can be described by an adiabatic approximation outside thin boundary layers around  $t = \pi/2 + N\pi$ , where methods of singular perturbation theory have been applied.

Finally, we present some observations on "chaotic" solutions at large  $\Gamma$  and  $0 \leq \Delta < 0.3$ . Outside the boundary layers,  $u(t)$  shows a regular behavior which is a damped anharmonic oscillation, slightly modified by the adiabatic law. However, in each of the boundary layers, the phase and the amplitude are suddenly changed in an apparently irregular way.

## 1. Introduction

We consider Duffing's equation [1,2] in the special case where the force does not have a term linear in  $x$

$$\ddot{x} + 2d\dot{x} + cx^3 = a \cos \omega t . \quad (1.1)$$

Since we are interested only in quantities invariant with respect to scale transformations  $x \rightarrow \alpha x$ ,  $t \rightarrow \beta t$ , two of the parameters  $d$ ,  $c$ ,  $a$ ,  $\omega$  can be chosen equal to 1. We shall start with  $c=a=1$  ( $\bar{x}' = d\bar{x}/d\bar{t}$ ):

$$\bar{x}'' + 2D\bar{x}' + \bar{x}^3 = \cos \Omega \bar{t} \quad (1.2)$$

and use later on  $c=\omega=1$

$$\ddot{x} + 2\Delta\dot{x} + x^3 = \Gamma \cos t . \quad (1.3)$$

The relation between the parameters and variables is

$$D = \Delta/\Gamma^{1/3} = \Delta\Omega , \quad \Omega = 1/\Gamma^{1/3} , \quad t = \Omega\bar{t} , \quad x = \bar{x}\Gamma^{1/3} . \quad (1.4)$$

Equations (1.2) and (1.3) are equivalent from a mathematical point of view. However, the decoupling from the external force ( $\Gamma \rightarrow 0$ ) is obviously easier to deal with in (1.3) than in (1.2) where one has to consider  $\Omega \rightarrow \infty$ , in particular in numerical calculations. Furthermore, it is convenient to have a fixed length of the period of the external force for investigations of the dependence of the shape of  $x(t)$  on the parameters and for Fourier analyses. On the other hand, (1.2) has the advantage to lead from a physical point of view to an ansatz for the solution in the adiabatic limit of small  $\Omega$ .

It is our aim to study in a large part of the parameter plane ( $\Gamma, \Delta$  or  $\Omega, D$ ) harmonic solutions, i.e. periodic solutions which

have the same frequency as the external force. The starting point is a quasistatic approximation which follows immediately if one considers the moving potential well belonging to the force in (1.2) in the limit of small  $\Omega$

$$V(x,t) = \frac{1}{4} x^4 - x \cos \Omega t . \quad (1.5)$$

The shape of this potential at  $t=0$  is shown in Fig.1.1.

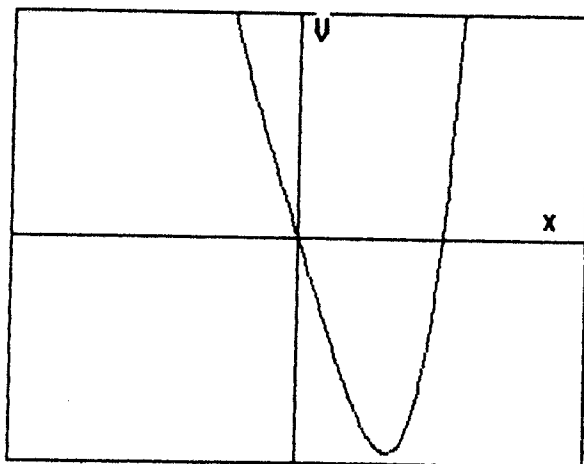


Fig.1.1 Shape of the potential (1.5) at  $t=0$ .

For small values of  $\Omega$ , the potential well generally moves slowly, so one can apply a quasistatic approximation:

$$x(t) = x_{\min}(t) + x_{\text{osc}}(t) ; \quad x_{\min}(t) = (\cos \Omega t)^{1/3} , \quad (1.6)$$

where  $x_{\min}(t)$  is the location of the minimum of the potential well (1.5) and  $x_{\text{osc}}(t)$  describes a damped oscillation around the minimum. The frequency of this oscillation is independent of  $\Omega$  and therefore becomes large in comparison with  $\Omega$  as one approaches the adiabatic limit. An estimate for the decrease of the oscillation amplitude during a half period  $T_A/2 = \pi/\Omega$  of the external force is given by a factor  $\exp(-DT_A/2)$ .

Let us consider for simplicity the case where  $\exp(-DT_A/2) \ll 1$ , i.e. the particle is sitting at the minimum for some time before  $x_{\min}(t)$  changes its sign at  $t=T_A/4+NT_A/2$ ,  $N$  integer. At these values of  $t$  the velocity  $\dot{x}_{\min}$  is infinite. Due to inertia and damping, the particle cannot follow immediately. So it finds itself in the moving potential well high above the location of the minimum and starts a new damped oscillation. This remark shows that the above description of the motion has to be supplemented by a special calculation for the small time interval during which  $|\dot{x}_{\min}|$  is large. One obtains in particular the height of  $x_{\text{osc}}(t)$  at the beginning of a new half period of the external force in addition to the frequency, which follows already from the potential (1.5).

This simple picture is qualitatively confirmed by a numerical evaluation of the Duffing equation. Fig.1.2 shows a harmonic solution for  $\Omega = 0.02$ .

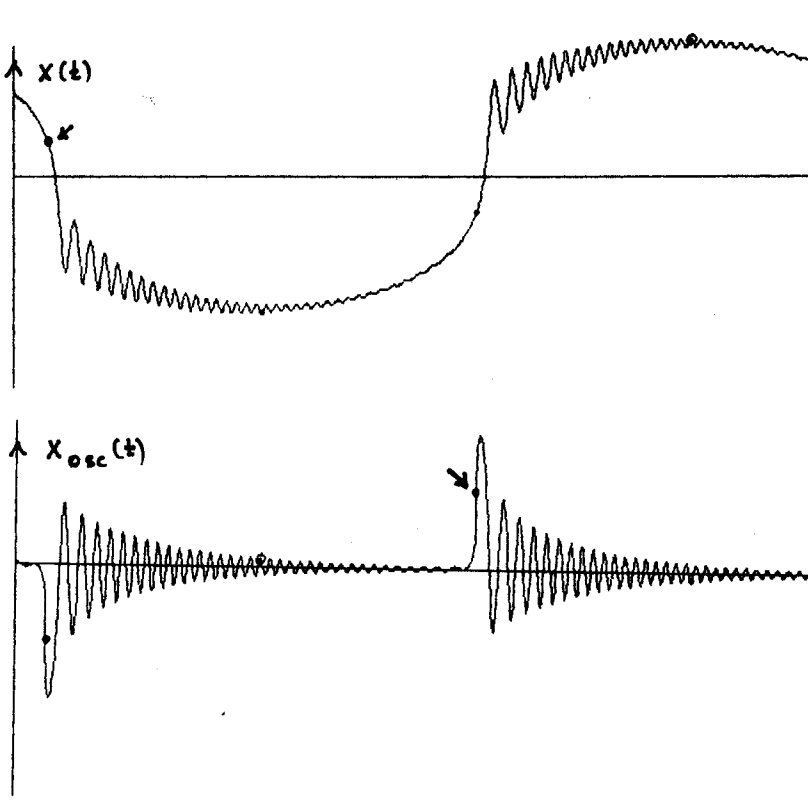


Fig.1.2:  $x(t)$  and  $x_{\text{osc}}(t)$  for  $\Omega = 0.02$ ,  $D = 0.025$ . The arrows point to the amplitudes belonging to  $t=T_A/4$ .

All numerical calculations have been carried out on a personal computer IBM AT, using the 4th order Runge-Kutta or the 4/5 Runge-Kutta-Fehlberg method. As a check of the reliability, the calculation was repeated if this seemed necessary with a smaller step size. The duration of a calculation is in general of the order of a minute, if one uses the mathematical coprocessor and Turbo-BASIC.

Our aim is twofold:

- i) to derive asymptotic expressions for the harmonic solutions in the limit  $\Gamma \rightarrow \infty$  under different assumptions on  $\Delta(\Gamma)$ ,
- ii) to determine the region in the  $\Gamma, \Delta$ -plane where the harmonic solutions can be described by approximations derived from an improved version (5.1) of the superposition (1.6).

We start in §2 by approximating the potential well (1.5) near its minimum by a parabola and treating quasistatically the motion in its neighborhood. The behavior of the solution near the times where  $\dot{x}_{\min}$  is infinite is treated in §3 in the special case where the damping is so large that the inertia term  $\ddot{x}$  in (1.3) can be ignored. This leads to the relaxation equation (3.3) which depends only on  $\rho = \Gamma^{2/3}/2\Delta$ . Using singular perturbation theory, we obtain an approximation which approaches uniformly the exact behavior in the limit of large  $\rho = \Gamma^{2/3}/2\Delta$ . The results are checked by numerical calculations in §4.

In §5 we introduce a new form of the Duffing equation, which is a differential equation for  $u(t) = x(t) - x_r(t)$ , where  $x_r(t)$  is the exact solution of the relaxation equation. In §6, using numerical evaluations, the magnitude and the  $t$ -dependence of the various terms in the equation for  $u(t)$  is discussed in different parts of the  $\Gamma, \Delta$ -plane and support is given to the simple superposition (1.6). In §7 we discuss the asymptotic behavior of the harmonic solutions for large  $\Gamma$ ,  $\Delta = \Gamma^\alpha$ ,  $\alpha > 1/4$ , and argue that a linear approximation to (5.3) is valid in this domain. In §8 we

discuss the domain  $\Delta \ll \Gamma^{1/4}$  and the asymptotic expression for the periodic solution in this region. Finally, we add some remarks on the Fourier expansion (§9). A summary is given in §10.

## 2. The quasistatic and parabolic approximation

The potential belonging to the force in (1.3)

$$V(x, t) = \frac{1}{4} x^4 - x\Gamma \cos t . \quad (2.1)$$

has its minimum at

$$x_{\min}(t) = (\Gamma \cos t)^{1/3} , \quad V_{\min}(t) = - \frac{3}{4} (\Gamma \cos t)^{4/3} . \quad (2.2)$$

We use the parabolic approximation

$$V(x, t) \approx V_{\min}(t) + \frac{3}{2} x_{\min}^2 (x - x_{\min})^2 \quad (2.3)$$

and find for the frequency of the oscillations in the potential well, neglecting its motion

$$\omega_{\text{osc}}^2 = 3x_{\min}^2 = 3 \Gamma^{2/3} (\cos t)^{2/3} - \Delta^2 . \quad (2.4)$$

The number of oscillations in a period  $2\pi$  of the external force is estimated from the average of  $\omega_{\text{osc}}$  over this interval, neglecting  $\Delta^2$  which is justified if  $\Gamma$  is large:

$$n_{\text{osc}} \approx \omega_{\text{av}} = 1.42 \Gamma^{1/3} . \quad (2.5)$$

The damping leads to a decrease of the amplitude of  $x_{\text{osc}}$  by a factor of  $\exp(-\pi\Delta)$  in a half period of the external force which agrees with Fig.1.2. As noticed earlier, the amplitude of the oscillation cannot be determined from these considerations.

For a quantitative test of the simple approximation we have calculated the number of oscillations per period  $2\pi$  by counting the number of zeros of  $\dot{x}(t)$  per half period in a harmonic solution of the Duffing equation, using a numerical evaluation. Table 2.1 shows that the result is more accurate than expected.

$\Gamma$	$n_{osc}$	$n_{osc}/\Gamma^{1/3}$
$10^7$	305	1.41
$10^6$	141	1.41
$10^5$	65	1.40
$10^4$	29	1.35

Tab.2.1: The dependence of the experimental number of oscillations per period on  $\Gamma$  for  $\Delta=0.5$ . The prediction for the value in the last column is 1.42 from the average of  $\omega_{osc}$  at large  $\Gamma$ . An average of  $\omega_{osc}^2$  gives the factor 1.46.

If we keep  $\Gamma = 10^6$  fixed and consider increasing values of the damping parameter  $\Delta$ , we expect a continuous transition to a relaxation process if  $\Delta$  reaches the order of  $\omega_{av}$ . Then the particle approaches the bottom of the potential well without oscillations. The  $\ddot{x}$ -term in the differential equation becomes negligible.

A further increase of the damping parameter leads to a motion in which the decomposition (1.6) is not useful any more. Instead, one has forced oscillations of a particle in a small  $x$ -range where the  $x^3$ -term in the differential equation is almost negligible. It plays a role mainly in the initial value problem, where it forces the center of the oscillation to move slowly to the origin.

We show in Fig.2.1 how the phase portrait depends on  $\Delta$  at fixed  $\Gamma=10^6$ . If  $\Delta$  reaches the order of  $10^4$ , the shape of the phase portrait approaches a circle and  $x(t) \approx -\Gamma/2\Delta \sin t$  (see eq. (3.3)).

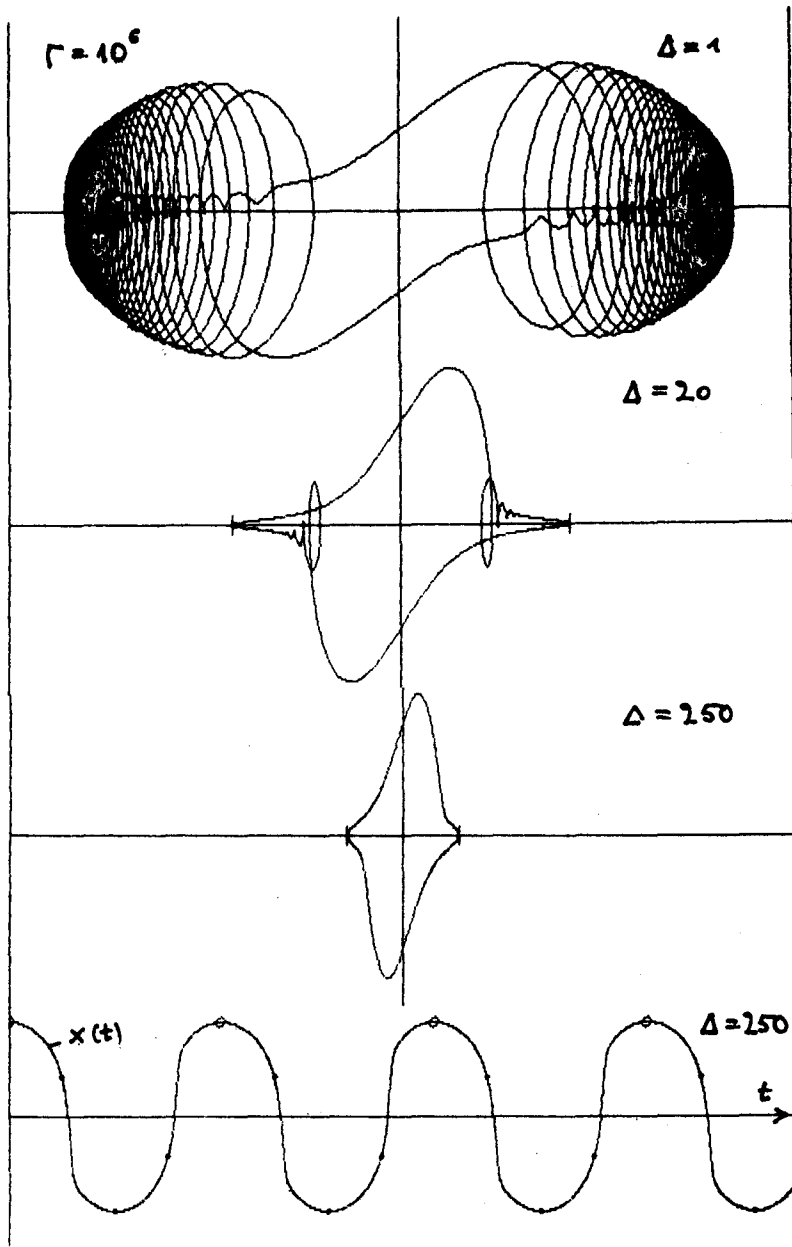


Fig.2.1: Phase portraits for harmonic oscillations at  $\Gamma=10^6$  and increasing values of  $\Delta$ . A suitable scale factor was used for the ordinate. The bottom figure shows the shape of  $x(t)$  for  $\Delta=250$ .



Another graphic representation of the motion in the parameter range where the present approximation can be applied is a plot of the energy  $E(t)$  versus  $x$ , where

$$E(t) = \frac{v^2}{2} + V(x,t) \quad (2.6)$$

and  $V(x,t)$  is the potential (1.5). If  $\Delta=0$ ,  $E$  is the value of the Hamilton function and one can calculate the adiabatic invariant (see §7).

Figure 2.2 shows the potential at  $t=0$  and  $\pi$ , the path of  $x_{min}$  and the curve belonging to the harmonic solution. One can clearly see the damped oscillation. The intersection of this curve with the ordinate occurs at an energy small in comparison with  $|V_{min}|$  if  $\Gamma$  is large.

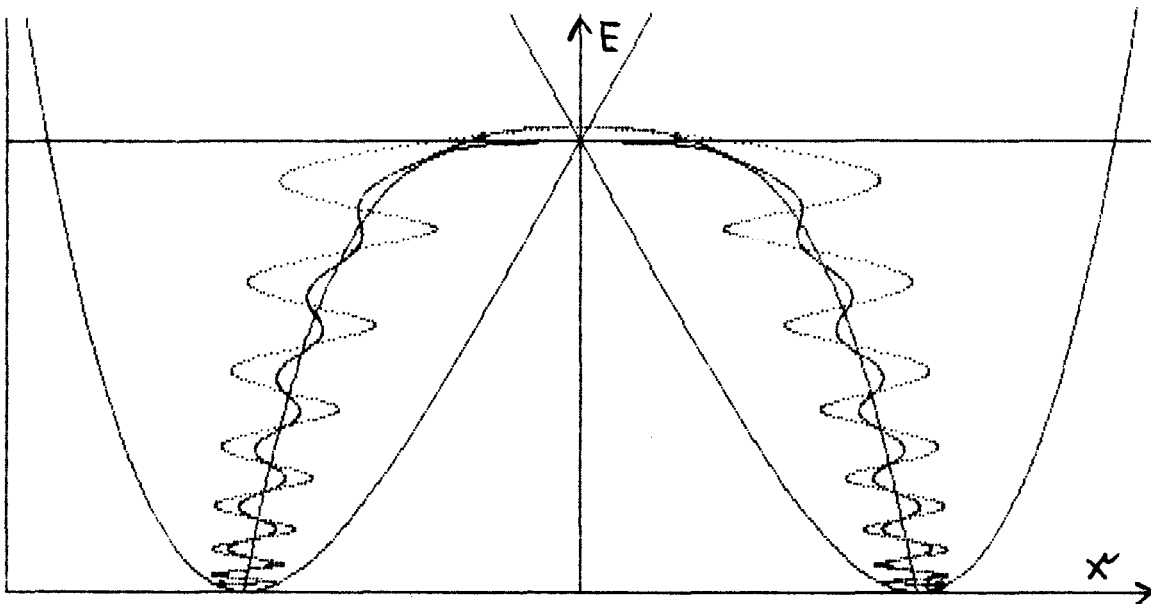


Fig.2.2: Plot of the energy  $E(t)$  vs.  $x$ , eq.(2.6), for a harmonic solution.  $\Gamma=10^4$ ,  $\Delta=0.75$ .

### 3. Harmonic solutions of the relaxation equation

We start our systematic investigation of the Duffing equation by considering a region where the effect of the  $\ddot{x}$ -term in the differential equation (1.3) is small or negligible.

The scale transformation

$$x(t) = \Gamma^{1/3} y(t) \quad (3.1)$$

leads to the differential equation

$$\frac{\ddot{y}}{2\Delta} + \dot{y} = \rho(\cos t - y^3) , \quad \text{where } \rho = \frac{\Gamma^{2/3}}{2\Delta} . \quad (3.2)$$

For constant values of  $\rho$  and increasing  $\Delta$ , it can be expected that the "inertia" term with the second derivative becomes negligible in the steady state, although it is always important in an initial value problem. In this paragraph, we shall neglect this term and consider the relaxation equation

$$\frac{\dot{y}_r}{\rho} = \cos t - y_r^3 ; \quad x_r(t) = \Gamma^{1/3} y_r(t) . \quad (3.3)$$

The effect of the inertia term will be discussed in §4.

Equation (3.3) shows immediately an important property: in the region of the  $\Gamma, \Delta$ -plane where the approximation is valid, the shape of  $x_r(t)$  and of the phase portrait depend only on the combination of  $\Gamma$  and  $\Delta$  which enters  $\rho$ . This is a scaling law.

Next we consider large values of  $\rho$ . Equation (3.3) suggests that the term  $\dot{y}/\rho$  on the left hand side may be neglected and the solution approaches the shape

$$y_{\infty}(t) = (\cos t)^{1/3}, \quad x_{\infty}(t) = (\Gamma \cos t)^{1/3} = x_{\min}(t). \quad (3.4)$$

As discussed in §1, this cannot be a good solution at all  $t$ , because the particle would have an infinite velocity when  $x_{\min}$  changes sign.

Therefore, it is necessary to discuss the solution of (3.3) for large  $\rho$  more carefully, applying the methods of singular perturbation theory [3].

There is no objection against the solution (3.4), except in small time intervals around the zeros of  $y_{\infty}$  which are called the boundary layers. We shall derive in this range a more accurate solution, which joins smoothly to the solution (3.4) outside this interval.

In order to have a simple notation, we introduce a shift of the time scale by  $3\pi/2$ , such that  $\cos t$  is replaced by  $\sin t$ . Furthermore, we consider only the time interval around the boundary layer at  $t=0$ . Since, for large  $\rho$ , the boundary layer is very thin,  $\sin t$  can be replaced by  $t$ .

Now, instead of (3.3) we have to study

$$\dot{y}_r = \rho(t - y_r^3) \quad (3.5)$$

in the boundary layer for large values of  $\rho$ .

The method starts with a scale transformation

$$t = \tau/\rho^{1/3}, \quad y_r = \eta/\rho^{1/3}. \quad (3.6)$$

Since we consider large values of  $\rho$ , the transition from the boundary layer to the range where (3.4) is used occurs in the

asymptotic region of  $\tau$ . The transformation (3.6) eliminates  $\rho$ , so we arrive with  $\eta' = d\eta/d\tau$  at

$$\eta' = \tau - \eta^3 . \tag{3.7}$$

The problem is to find a solution  $\eta(\tau)$  of this equation which behaves as  $\tau^{1/3}$  for  $\tau \rightarrow \pm\infty$  and can therefore smoothly join the solution  $y_\infty = (\sin t)^{1/3}$  (i.e. (3.4) with the shift of the time scale).

Although (3.7) looks simple, it can be solved only numerically. It turns out that all solutions fulfill the boundary condition for  $\tau \rightarrow \infty$ . However, for  $\tau \rightarrow -\infty$  almost all solutions go much more rapidly to  $\infty$  or  $-\infty$  and only one solution has the correct behavior. Figure 3.1 shows the shape of this solution and Table 3.1 gives the values of its parameters.

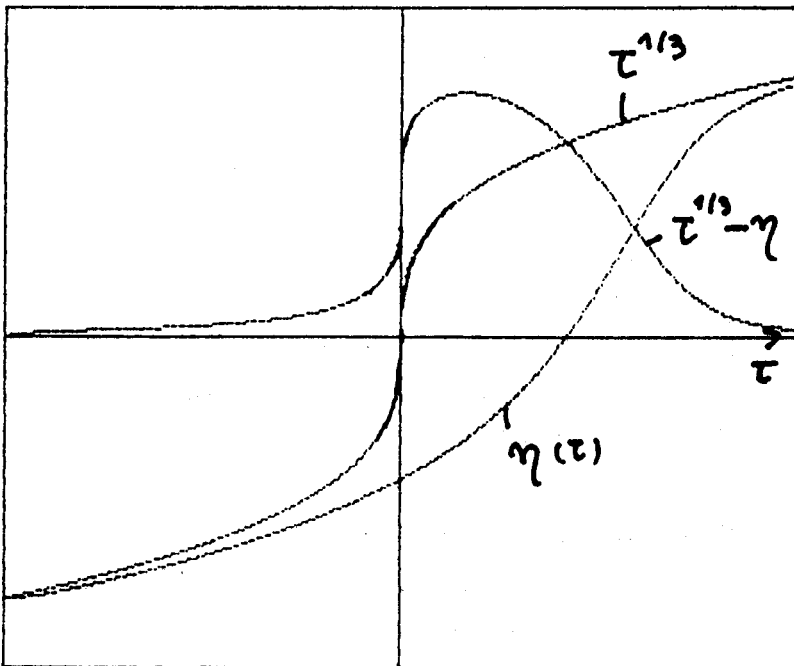


Fig.3.1: Solution  $\eta(\tau)$  of the boundary value problem of (3.7) and related curves.

$$\begin{aligned}
 \eta(0) &= -0.752137, \quad \eta(1.095) = 0 \\
 \eta'(0) &= 0.42549, \quad \eta'_{\max} = 1.365 \text{ at } \tau = 1.45 \\
 (\tau^{1/3} - \eta)_{\max} &= 1.292 \text{ at } \tau = 0.43 \\
 &\text{decrease to } 1/10 \text{ at } \tau = -0.59 \text{ and } +2.14 \\
 \eta''/\eta' &: \max = 0.988 \text{ at } \tau = 0.89, \min = -2.27 \text{ at } \tau = 2.12 \\
 \eta'' &: \max = 1.00 \text{ at } \tau = 1.095, \min = -1.72 \text{ at } \tau = 1.90
 \end{aligned}$$

Tab.3.1: Parameters of the solution of the boundary value problem of (3.7).

Now we go back to our old time scale and time origin and make the following ansatz for the improved solution of (3.3) for large  $\rho$  [3].

$$\begin{aligned}
 y_r^0(t) &= (\cos t)^{1/3} - (t-3\pi/2)^{1/3} + y_c(t) \\
 &\equiv (\cos t)^{1/3} + y_a(t),
 \end{aligned} \tag{3.8}$$

where

$$y_c(t) = \rho^{-1/3} \eta [\rho^{1/3}(t-3\pi/2)]. \tag{3.9}$$

Within the thin boundary layer at  $t \approx 3\pi/2$ , the first two terms in (3.8) cancel each other, so the solution is given by  $y_c(t)$ . Outside the boundary layer we are in the asymptotic range of  $\eta(\tau)$ , so the last two terms in (3.8) cancel each other and  $y_r = y_\infty$ .

Equation (3.8) solves the problem approximately only in the neighborhood of one of the boundary layers. An approximation to the periodic solution of the relaxation equation (3.3) is given by

$$y_r(t) = \sum_{-\infty}^{\infty} y_a(t-2n\pi) - \sum_{-\infty}^{\infty} y_a(t-(2n+1)\pi) + (\cos t)^{1/3}. \tag{3.10}$$

It can be shown that the sums converge and that in the neighborhood of the transition points the corrections are in fact of the order  $1/\rho$ .

The approximation (3.10) is valid at least up to the order  $\rho^{-7/11}$ . It fulfills the differential equation (3.3) uniformly at least up to the order  $\rho^{-9/11}$ . A numerical test shows that the approximation is very good for  $\rho \geq 50$ . At  $\rho=10$  one can see in a plot on the screen that the two solutions do not join well, because the approximation  $\cos t \approx t - 3\pi/2$  is not valid with sufficient accuracy in an interval  $\Delta t = 1/\rho^{3/5}$  around  $t = 3\pi/2$ .

Figure 3.2 shows examples for the shape and the width of the correction  $x_r(t) - x_\infty(t)$ , which have been determined by a numerical evaluation. Except for the scale, the curves agree with the curve for  $\tau^{1/3} - \eta$  in Fig.3.1.

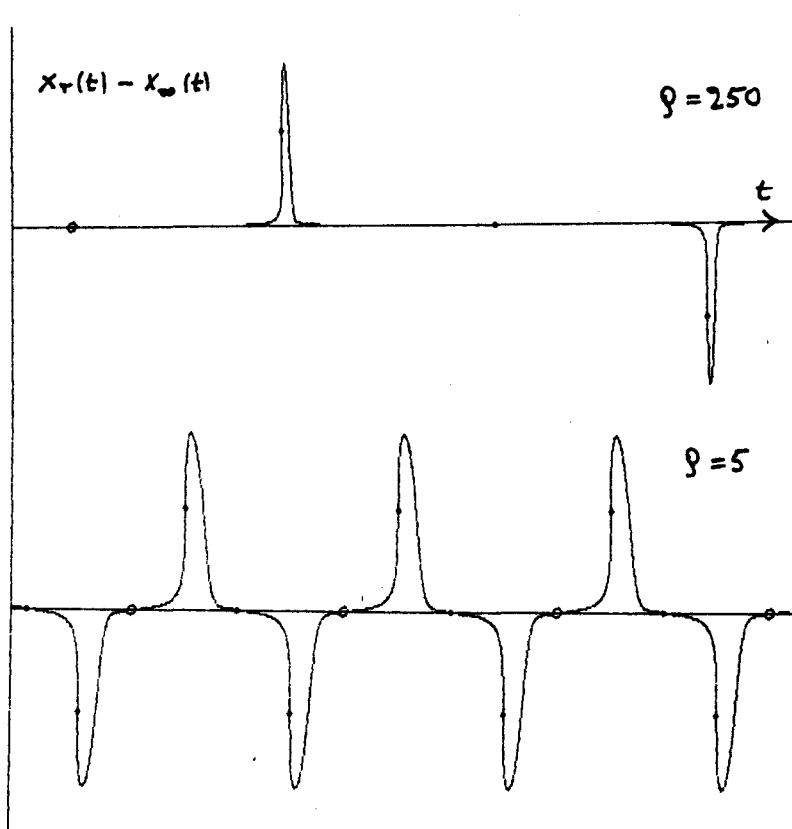


Fig.3.2:  $x_r(t) - x_\infty(t)$  at  $\rho=250$  and 5.

According to Tab.3.1, the width of the peak in the boundary layer (defined by a decrease to 1/10 of its height) behaves as

$$\Delta t_b = 2.7/\rho^{3/2}, \quad (3.11)$$

whereas the height goes as

$$|y_r - y_\infty|_{\max} = 1.29/\rho^{1/2}. \quad (3.12)$$

The maximum is attained in the boundary layer. Well outside the boundary layer it is true that  $y_r - y_\infty = O(1/\rho)$ , so that the difference  $y_r - y_\infty$  shows sharp needles as a function of  $t$ , near  $t = (2N+1)\pi/2$ . The convergence of  $y_r$  to  $y_\infty$  is thus not of uniform quality as  $\rho$  goes to infinity.

#### 4. Test of the accuracy of the approximation to the relaxation equation

In order to test our application of singular perturbation theory by a numerical evaluation, we have selected five sensitive quantities in the boundary layer:

- a. the velocity  $\dot{y}_r(3\pi/2)$  and the maximum of the velocity  $\dot{y}_{r_{\max}}$ , which are infinite in the approximation  $y_\infty(t)$ ;
- b. the maximum of the correction  $|y_r(t) - y_\infty(t)|$ ;
- c.  $y_r(3\pi/2)$  and the time when  $y_r$  passes zero.

Table 4.1 shows the values obtained from a numerical solution divided by the results derived from singular perturbation theory. As expected the agreement is improving for increasing values of  $\rho$ . The last column shows that  $y_{r_{\max}}$  starts to decrease at about  $\rho=5$ . At fixed  $\Gamma$  and increasing  $\Delta$  this corresponds to the transition to the case of small oscillations mentioned in §2.

$\rho$	$\dot{y}_r(3\pi/2)$	$\dot{y}_{r_{max}}$	$[y_r - y_{\infty}]_{max}$	$\bar{t}(y_r=0)$	$y_r(3\pi/2)$	$y_{r_{max}}$
100.0	0.9998	0.9974	0.9991	0.9993	0.9999	1.00
10.0	0.9967	0.9802	0.9992	1.0024	0.9989	1.00
5.0	0.9922	0.9562	0.9984	1.0062	0.9974	1.00
1.0	0.8615	0.7104	0.9784	1.0390	0.9505	0.85
0.5	0.1864	0.4831	0.8146	0.8970	0.5712	0.50

Tab.4.1: Ratio of the numerical result derived from (3.3) and the prediction from the approximation (3.8).  $\bar{t}=t-3\pi/2$ .

### 5. A new form of the Duffing equation

It is now our aim to derive a new differential equation which is equivalent to the Duffing equation (1.3). The result looks more complicated, but it has the advantage to include an exact version of the superposition (1.6) which was based on an intuitive argument.

We define  $u(t)$  by

$$u(t) := x(t) - x_r(t) , \quad (5.1)$$

where  $x_r(t)$  is a solution of the relaxation equation

$$2\Delta\dot{x}_r + x_r^3 = \Gamma \cos t . \quad (5.2)$$

If the ansatz (5.1) for  $x(t)$  is inserted into the Duffing equation (1.3), one obtains a differential equation for  $u(t)$

$$\ddot{u} + 2\Delta\dot{u} + u(3x_r^2 + u^2) + 3x_ru^2 = -\ddot{x}_r := f(t) . \quad (5.3)$$



Since  $x_r(t) \approx x_\infty(t)$  outside the boundary layers, we might just have used the latter. However, it will turn out that in large domains of the parameter plane the equation for  $u(t)$ , as defined in (5.1), admits indeed of periodic solutions of uniformly small magnitude (see §7). As a comparison to (5.2), the differential equation satisfied by  $x_\infty(t)$  is

$$\ddot{x}_\infty = -\frac{1}{9}x_\infty - \frac{2}{9}\Gamma^2 x_\infty^{-3}, \quad (5.4)$$

which is highly singular at  $x_\infty=0$ .

Equation (5.3) has the disadvantage that it contains the function  $x_r(t)$  which is known only numerically. But for a given value of  $\rho$  the periodic solution of the relaxation equation is uniquely defined and (5.3) is then exactly equivalent to the Duffing equation (1.3). Equation (5.3) suggests possibilities for approximations which one would not guess directly from the original equation.

From a mathematical point of view, (5.3) is of the type of Hill's equation, generalized by a damping term, two nonlinear terms and an external force  $f(t)$ .

In a steady state, the nonlinear  $u$ -oscillator (5.3) is excited in two ways:

a. By the periodic external force  $f(t) = -\ddot{x}_r$ . It will be shown that in a large part of the  $\Gamma, \Delta$ -plane the dominant contribution to  $f(t)$  consists of two narrow impulses of opposite signs in the boundary layers (Fig.6.2).

b. By the time dependence of the coefficients, in particular in the term  $3x_r^2(t)u$ .

The shape of  $f(t)$  can be calculated from  $\eta(\tau)$  and (3.9) in the region of the parameter plane, where the approximation (3.8) is

valid. Near  $t=3\pi/2$  the peak and the dip have the magnitudes  $1.0(\Gamma/2\Delta)$  and  $-1.72(\Gamma/2\Delta)$ , respectively, and the time difference is  $\Delta t=0.81/\rho^{3/2}$ . Since  $\eta' \approx \frac{1}{2}\tau^{-3/2} \rightarrow 0$  as  $\tau \rightarrow \pm\infty$ , the integral over  $\eta''$  over all  $\tau$  is zero, i.e. the areas under the broad bump and the narrow dip are the same. This result suggests to approximate  $f(t)$  by a  $\delta'$ -function. However, it turns out that the term  $-3x\dot{x}u$  has a zero at the dip of  $f(t)$  and is very rapidly varying in the neighborhood, so it is not useful to approximate  $f(t)$  by  $\delta'(t)$ .

It will be of interest to study the effects of both excitations in the resonance region. Figure 5.1 shows the time dependence of the excitation  $f(t)$  and the response  $u(t)$  for parameters in the range of the superharmonic branch of the second resonance, for which the coefficient of the second term of the Fourier expansion is larger than that of the first term. This resonance is discussed in detail in [1,2]. The structure of  $f(t)$  would be even narrower for smaller values of  $\Delta$ . It might be useful to study the connection between the treatment of resonances in terms of the  $u$ -oscillations and by the method of Parlitz and Lauterborn [4].

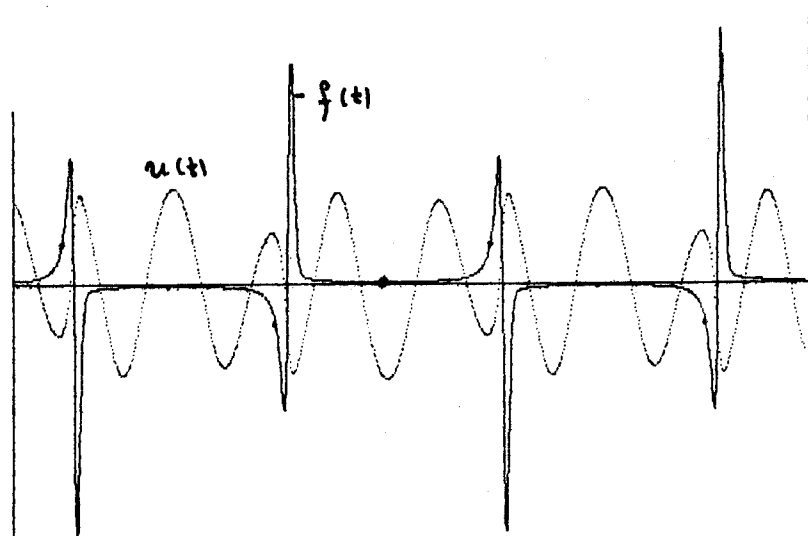


Fig. 5.1:  $f(t)$  and  $u(t)$  for the superharmonic solution at  $\Gamma=17$ ,  $\Delta=0.1$  corresponding to  $\rho \approx 66$ .

In Fig.5.2 we show that the exact solution  $x(t)$  appears as a superposition of a background  $x_r(t)$  and an oscillation  $u(t)$  even for the relatively small value  $\Gamma=17$ .

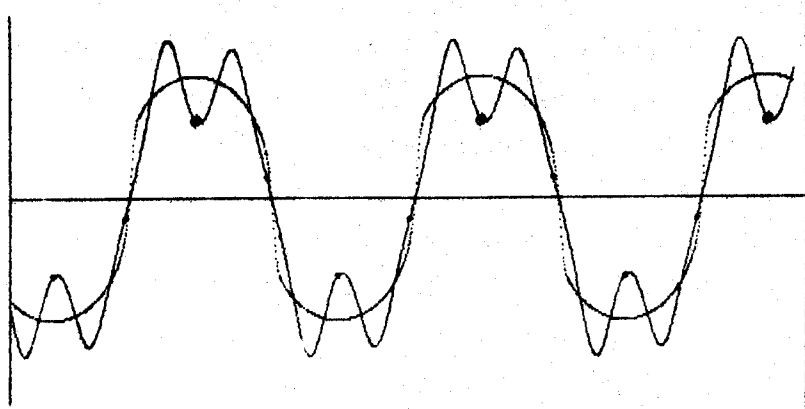


Fig.5.2: The oscillation of  $x(t)$  around the background  $x_r(t)$  for the solution shown in Fig.5.1.

#### 6. Numerical study of the equation for $u(t)$ at $\Gamma=10^6$

In order to get information on the magnitude of the various terms in (5.3) at a fixed large value of  $\Gamma$  and different values of  $\Delta$ , we have performed numerical calculations. Figure 6.1 shows the different terms at  $\Gamma=10^6$ ,  $\Delta=50$ , which belongs to  $\rho=100$ . All terms are appreciably different from zero only in the range of the boundary layer. It is seen that all linear terms are of comparable magnitude. In particular, the ratio of the maxima of  $\ddot{u}$  and  $2\Delta\dot{u}$ , which goes to zero for large  $\Delta$ , is about 1/2. The maximum of the nonlinear term  $3x_r u^2$  is only 1/8 of the maximum of  $3x_r \dot{u}$  and  $u^2$  is still smaller. The maximum of  $u(t)$  is 1/20 of the maximum of  $x_r(t)$ . Neglecting the force  $f(t)$  outside the boundary layers is justified since it turns out to be about 500 times smaller than the maximum of  $f(t)$  within the boundary layers.

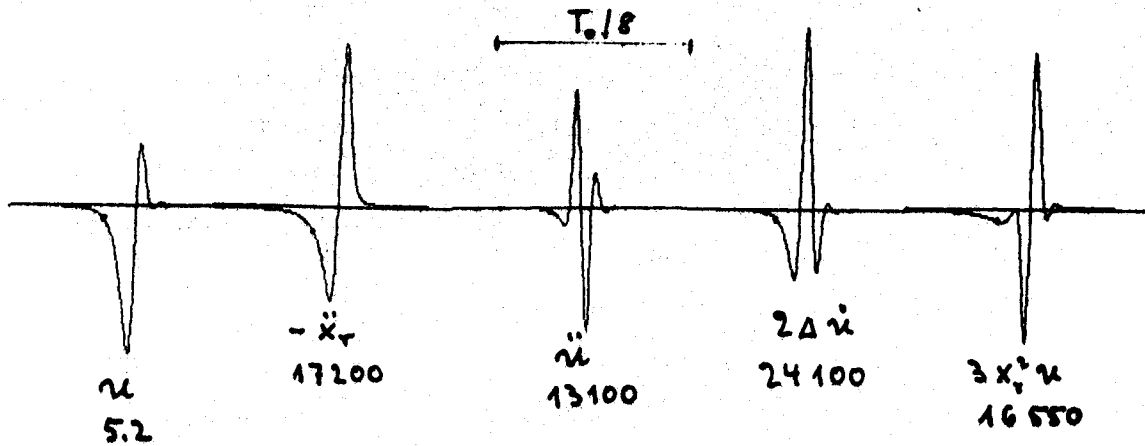


Fig.6.1: Structures of the terms in (5.3) at  $\Gamma=10^6$ . The  $t$ -scale is the same in all cases. The numbers give the magnitude of the maxima. The maximum of the largest nonlinear term  $3x_r^2u$  is 2110.

Figure 6.2 shows the force  $f(t)$  and the response  $u(t)$  at fixed  $\Gamma=10^6$  and  $\Delta$  between 4 and 100. At  $\Delta \geq 50$  both have qualitatively the same shape. As  $\Delta$  becomes smaller,  $u(t)$  shows damped oscillations which enter the  $t$ -region between the boundary layers and are visible even at the end of a half period at  $\Delta \approx 0.8$  (similar to Fig.1.2). The width of the structure of  $f(t)$  decreases in agreement with the estimate in §5.

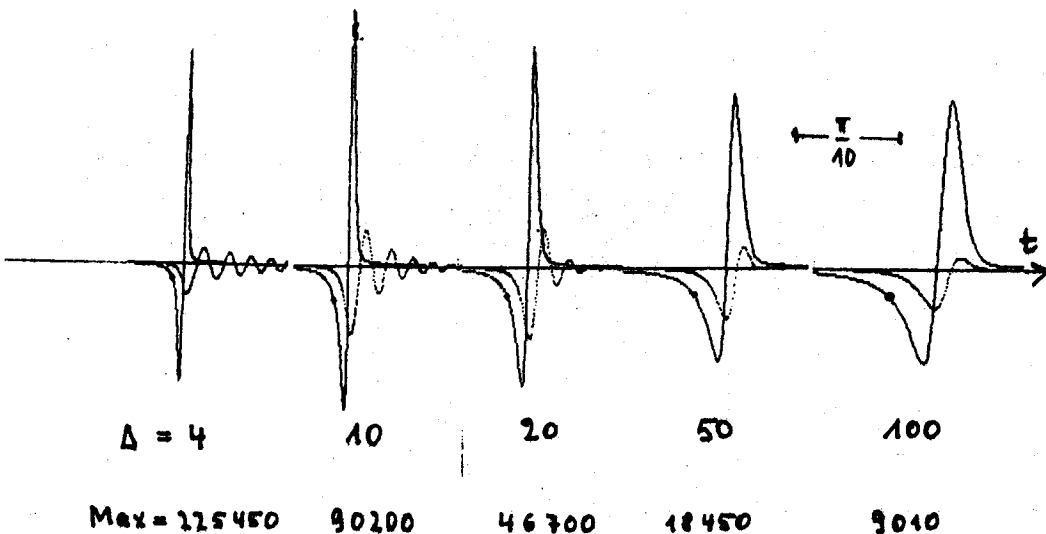


Fig.6.2:  $f(t) = -\ddot{x}_r$  near  $t=3\pi/2$  at  $\Gamma=10^6$  and  $\Delta$  from 4 to 100. The dotted line shows  $1024 u(t)$ . The  $t$ -scale is the same in all cases.

The dip of  $u(t)$  is a consequence of the fact that the particle cannot follow the rapid motion of the minimum when it passes the origin. The bump has a contribution from the attraction towards the new location of the minimum and another one from the rapid change of the potential.

Fig.6.3 shows a comparison between  $u=x-x_r$  and  $x-x_{\infty}$  for  $\Gamma=10^6$ . At  $\Delta=100$  which belongs to  $\rho=50$ ,  $u$  is much smaller than  $x-x_{\infty}$ , i.e.  $x_r$  is a much better approximation to the exact solution  $x(t)$  than  $x_{\infty}$ . At  $\Delta=4$  the two curves are near to each other in the boundary layer as expected because of the large value  $\rho=1250$ . They agree very well in the range of the oscillations.

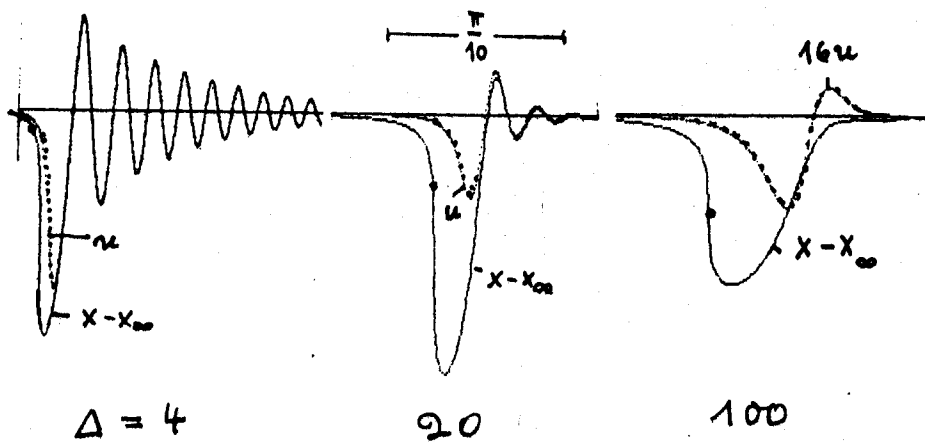


Fig.6.3: Comparison between  $x(t)-x_{\infty}(t)$  and  $u(t)$  at  $\Gamma=10^6$  and  $\Delta$  from 4 to 100. The agreement is very good in the range of the oscillations. The  $t$ -scale is the same in all cases.

Since we shall study the linearized version of (5.3) in §7.1, it is of interest to determine the magnitude of the maxima of the nonlinear terms as a function of  $\Delta$  at fixed  $\Gamma=10^6$ . In Table 6.1 we have divided these values by the maximum of  $|\ddot{x}_r|$  in order to reduce the variation.

$\Delta$	100	50	20	10	5
$\rho$	50	100	250	500	1000
$2\Delta\dot{u}$	1.41	1.40	0.79	0.29	0.08
$\ddot{u}$	0.27	0.76	1.45	1.38	1.23
$3x_r^2u$	0.69	0.96	1.18	0.86	0.62
$3x_ru^2$	0.035	0.12	0.43	0.60	0.46
$u^3$	0.001	0.009	0.07	0.16	0.15

Tab.6.1: The maxima of various terms in (5.3) at  $\Gamma=10^6$  and different values of  $\Delta$  divided by the maximum of  $|\ddot{x}_r|$ .

As expected, the nonlinear terms are negligible at large  $\Delta$ . The leading nonlinear term becomes important at about  $\Delta \leq 20$ . Figure 6.4 shows a comparison between the linear term  $3x_r^2u$  and the nonlinear terms as a function of time at  $\Gamma=10^6$ ,  $\Delta=10$ . Since  $u$  is small in comparison with  $x_r$ , the nonlinear terms are important only in the boundary layer and the first oscillations, since they decrease more rapidly than  $u(t)$ .

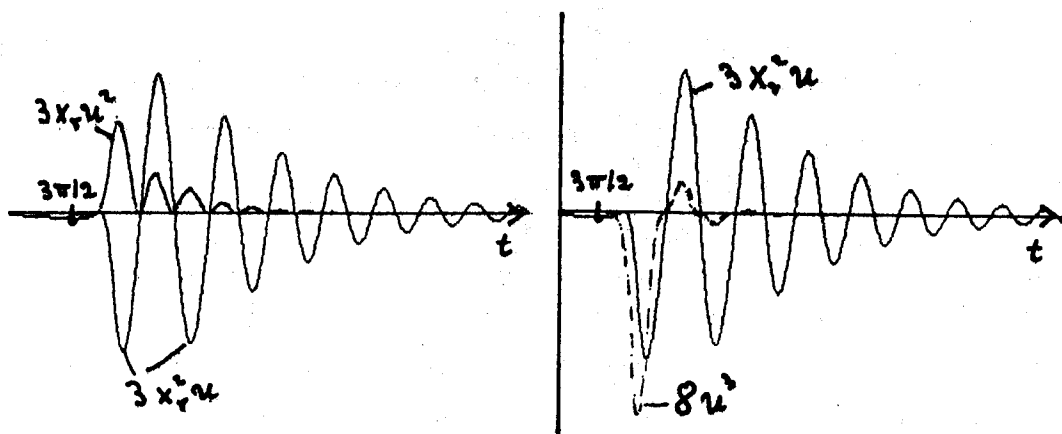


Fig.6.4: Comparison of the nonlinear terms in (5.3) with  $3x_r^2u$  at  $\Gamma=10^6$ ,  $\Delta=10$ .

## 7. Approximations to the new form of the Duffing equation

### 7.1 The relaxation approximation $u(t) \approx 0$

First, we consider a fixed large value of  $\Gamma$  and increasing values of  $\Delta$ . The above discussion shows that  $f(t)$  is decreasing, so we expect that  $u(t)$  becomes smaller and the exact solution  $x(t)$  approaches  $x_r(t)$ . This corresponds to the statement that the inertia term  $\ddot{x}$  in the Duffing equation becomes negligible.

We estimate the importance of  $\ddot{x}$  in comparison with  $2\Delta\dot{x}$  by calculating the ratio  $\ddot{x}_r/2\Delta\dot{x}_r$ , which has its largest values in the boundary layer. Equation (3.6) leads to

$$v = \frac{\ddot{x}_r}{2\Delta\dot{x}_r} = \frac{\eta''}{\eta'} \frac{\Gamma^{2/5}}{(2\Delta)^{6/5}}. \quad (7.1)$$

We use the maximum of  $|\eta''/\eta'|$  as given in Table 3.1 and solve for  $\Delta$

$$\Delta = 0.83 \frac{\Gamma^{1/4}}{v^{5/6}}; \quad \Delta = 1.7 \Gamma^{1/4} \text{ for } v = 0.3. \quad (7.2)$$

One can expect that this curve in the  $\Gamma, \Delta$ -plane gives roughly a lower limit for the validity of the relaxation approximation as long as  $\Gamma$  is not too small.

Another means of obtaining the critical curve  $\Delta \approx \Gamma^{1/4}$  is offered by the scaling transformations used to establish the thickness of boundary layers (Ref.3, p.419). We start from (3.2), which is equivalent to the Duffing equation (1.3), perform again a shift of the time variable which leads to  $\sin t$  instead of  $\cos t$  on the right hand side, and consider small  $t$ -values, so  $\sin t$  can be

approximated by  $t$ . Then we write  $y=Y\mu$ ,  $t=T\delta$  and obtain

$$\frac{\mu}{\delta^2 \Gamma^{2/3}} \frac{d^2 Y}{dT^2} + \frac{2\Delta}{\Gamma^{2/3}} \frac{\mu}{\delta} \frac{dY}{dT} + \mu^3 Y^3 = T\delta. \quad (7.3)$$

If we choose  $\mu = \delta^{1/3}$  we expect that the reduced equation in  $T$ , following from (7.3) by letting  $\delta \rightarrow 0$ , has a solution with the asymptotic behavior  $Y(T) \sim T^{1/3}$ , so that it matches the solution  $(\sin t)^{1/3}$ , valid outside a small neighborhood of the origin. Next, we choose  $\delta$  so that

$$\frac{2\Delta}{\Gamma^{2/3}} \frac{\mu}{\delta} = O(1), \quad \delta = \left[ \frac{2\Delta}{\Gamma^{2/3}} \right]^{3/2}, \quad (7.4)$$

i.e. we balance the friction term in (7.3) against the two terms on its right. With this choice, the acceleration term is  $O(\Gamma/\Delta^4)^{1/6}$ , i.e. it is vanishingly small if  $\Delta$  increases quicker than  $\Gamma^{1/4}$ . Thus the boundary layer around  $t=0$  has a "thickness" of  $O(1/\rho^{1/6})$  with  $\rho$  of (3.2). The reduced differential equation describing the evolution in the boundary layer is obtained by letting  $\Gamma \rightarrow \infty$ : it is (3.7) with  $\eta \rightarrow Y$ .

Below the line  $\Delta = \Gamma^{1/4}$  we can only balance the acceleration term against  $Y^3$  and  $T$  and obtain a boundary layer of thickness  $O(1/\Gamma^{1/4})$ , independent of  $\Delta$ . Letting  $\Gamma \rightarrow \infty$ , the reduced differential equation for the boundary layer is

$$\ddot{Y} + Y^3 = T. \quad (7.5)$$

For a quantitative test of the approximation  $u(t) \approx 0$ , Tab.7.1 gives a comparison between results derived from numerical solutions of the Duffing equation and of the relaxation equation (3.3). Since the main difference is expected within the boundary layer, we compare again the ratios of the sensitive quantities used already in Tab.4.1.



		$\Delta$	$\rho$	$x(\frac{3\pi}{2})$	$v(\frac{3\pi}{2})$	$v_{\max}$	$t_{x=0} - \frac{3\pi}{2}$
$\Gamma=10^4$	$(\Delta=54)$	100	50	1.006	0.985	1.017	1.000
		50	100	1.016	0.957	1.031	1.075
$\Gamma=10^4$	$(\Delta=17)$	100	2.32	1.001	0.997	1.002	1.000
		46	5	1.002	0.992	1.010	1.013
		12	20	1.023	0.938	1.034	1.111
		5	46	1.068	0.840	0.978	1.323
$\Gamma=10^3$	$(\Delta=10)$	20	2.5	1.006	0.987	1.011	1.021
		10	5	1.015	0.964	1.026	1.062
		5	10	1.037	0.911	1.024	1.164

Tab.7.1: Ratios of sensitive quantities calculated from the Duffing equation and from the relaxation equation (3.3). The values in brackets in the second column are the estimates (5.2) for the  $\Delta$ -values below which the inertia term becomes important.

It is seen that the accuracy of the relaxation approximation behaves as expected from (7.2). In the  $\Gamma, \Delta$ -plane, the range of validity extends up to small values of  $\Gamma$ . In this region, the comparison can be made between the Fourier coefficients calculated from the numerical solutions of (1.3) and (3.3). A good agreement is found for  $\Delta \geq 2$ .

## 7.2 The linearized equation for the u-oscillator

We have seen in §7.1 that the approximation  $u(t) \approx 0$  is valid in the upper part of the  $\Gamma, \Delta$ -plane down to a curve which rises as  $\Gamma^{1/4}$  for large  $\Gamma$  and runs near  $\Delta=2$  for small  $\Gamma$ . One can expect that in the neighborhood of this boundary  $u(t)$  is still so small that the nonlinear terms in (5.3) can be neglected. Therefore, we shall discuss the linearized equation

$$\ddot{u} + 2\Delta\dot{u} + 3x_r^2 u = -\ddot{x}_r = f(t) . \quad (7.6)$$

As mentioned above, at large  $\rho = \Gamma^{\frac{2}{3}}/2\Delta$  the dominant contributions to  $f(t)$  are the two impulses in the thin boundary layers. Therefore, in the large time interval between the boundary layers, it is of interest to study (7.6) with  $f(t)=0$ . We apply the usual ansatz

$$u(t) = e^{-\Delta t} w(t) \quad (7.7)$$

and obtain a Hill equation

$$\ddot{w} + \omega_u^2(t)w = 0, \text{ with } \omega_u^2(t) = 3x_r^2(t) - \Delta^2, \quad (7.8)$$

where  $x_r$  is well approximated by  $x_{\infty} = x_{\min}$  (see (3.8)). Then,  $\omega_u^2$  agrees with  $\omega_{\text{osc}}^2$  in (2.4). The advantage in comparison with the intuitive ansatz in §2 is that we now have expressions for the force  $f(t)$  and for the difference between  $x_{\infty}$  and  $x_r$  in the boundary layer, which make it possible to calculate not only the time-dependent frequency of the  $u$ -oscillation but also its amplitude. The neglected nonlinear terms in  $u$  correspond to the corrections to the parabolic approximation in  $V(x,t)$ , eq.(1.5).

Instead of the quasistatic approximation (§2) we shall now discuss the parametric excitation and the damping in (7.8) in the adiabatic approximation, where the action, which is proportional to the energy  $E(t)$  divided by  $\omega_u$ , decreases as  $\exp(-2\Delta t)$  [7]. We consider the motion in an interval between the boundary layers at  $t = -\pi/2$  and  $\pi/2$  and find

$$u(t) = \frac{U e^{-\Delta t}}{\sqrt{\omega_u(t)}} \cos \left[ \omega_{\text{ad}}(t)t + \phi \right] \quad (7.9)$$

with

$$\begin{aligned} \omega_{ad}(t)t &= \sqrt{3} \Gamma^{1/2} \int_0^t (\cos t')^{1/2} dt' \\ &= \omega_u(t)t + \sqrt{3} \Gamma^{1/2} \int_0^t \frac{t' \sin t'}{(\cos t')^{3/2}} dt' . \end{aligned} \quad (7.9a)$$

For a detailed test, we have used a numerical solution of the Duffing equation in order to determine the time intervals  $\Delta t$  between adjacent zeroes with  $\dot{u} > 0$  of  $u(t)$ . We approximate  $\omega_{ad}$  by  $\omega_u$  and take the average of this frequency in each of the small time intervals. Then the prediction from (7.9) is  $\Delta t \approx 2\pi/\omega_u$ .

Table 7.2 gives the ratios of the numerical determinations of the time intervals to the predictions.

$\Gamma = 10^3$		$\Gamma = 10^4$		$\Gamma = 10^5$	
$\Delta t/\text{pred.}$	$U_{\max}$	$\Delta t/\text{pred.}$	$U_{\max}$	$\Delta t/\text{pred.}$	$U_{\max}$
1.007	1.74	1.003	2.41	1.003	4.48
1.007	1.75	1.003	2.42	1.003	4.48
1.007	1.76	1.003	2.42	1.002	4.48
		...	...	...	...
		1.004	2.44	1.006	4.48

Tab.7.2: Zeros of  $u(t)$  and heights of the maxima for harmonic oscillations at  $\Delta=0.3$  and various values of  $\Gamma$  in the range  $t=2\pi N \dots 2\pi N + \pi/2$ . We give the ratios  $\Delta t/(\omega_u/2\pi)$ , using only the first term in (7.9a) and the heights of the maxima expressed by the value of  $U$  in (7.9).

The numerical calculation shows that the oscillation of  $u(t)$  is asymmetric, i.e. the anharmonic terms are not negligible in our range of parameters  $\Gamma, \Delta$ . The magnitude of  $U_{\min}$  is larger, as expected from the shape of the potential belonging to eq.(5.3).

With  $U_{av} = (U_{max} + U_{min})/2$  we find  $(U_{min} - U_{max})/U_{av} = 0.10$  at  $\Gamma = 10^3$  and 0.06 at  $\Gamma = 10^4$ .

The corrections following from the adiabatic treatment lead to a constancy of  $U_{max}$  (Tab.7.2).

In [5], Byatt-Smith gives an equation for  $x - x_{\infty}$  in the limit of large  $\Gamma$  and fixed  $\Delta$  which agrees with (7.9) except for a factor  $\Gamma^{1/2}/\Gamma^{1/2}$  and an additional term in (7.9a). He uses this equation at  $\Gamma \approx 1000$ , where nonlinear effects are not yet negligible according to our results.

As  $\Gamma$  increases at fixed  $\Delta$ ,  $U_{av}$  is increasing but  $U_{av}/\Gamma^{1/2}$  is decreasing, and therefore the linear approximation becomes better. Assuming a power law, we find by a crude estimate in the range  $\Gamma = 10^3 \dots 10^4$  that  $U_{av}/\Gamma^{1/2}$  decreases as  $1/\Gamma^{1/2}$  in agreement with Byatt-Smith's formula.

### 7.3 The magnitude of $u(t)$ in the limit $\Gamma \rightarrow \infty$ , $\Delta = \Gamma^{\alpha}$

To ascertain the domains of parameter space where  $u(t)$  can be neglected for large  $\Gamma, \Delta$  we transform (5.3) to a nonlinear integral equation for  $u(t)$ :

$$u(t) = A(f, u)u_1(t) + B(f, u)u_2(t) - \int_0^t K(t, t') [3u^2(t')y_r(t') + u^3(t') + f(t')] dt' \quad (7.10)$$

where

$$K(t, t') = \frac{u_1(t)u_2(t') - u_1(t')u_2(t)}{u_1'(t')u_2(t') - u_1(t')u_2'(t')} \Gamma^{3/2} \quad (7.11)$$

The coefficients  $A(f,u)$ ,  $B(f,u)$  are determined so that the right hand side is a periodic function of  $t$ . The functions  $u_1(t)$  and  $u_2(t)$  are two independent solutions of the homogeneous part of (7.6). We may try to solve (7.10) by iteration; the first step is

$$u^{(1)}(t) = A(f,0)u_1(t) + B(f,0)u_2(t) - \int_0^t K(t,t')f(t')dt' \quad (7.12)$$

and the problem is to show that the sequence of iterates obtained in this manner is convergent to a quantity that is negligibly small for  $\Gamma, \Delta$  large enough. In particular  $u^{(1)}(t)$  must be bounded by quantities that tend to zero as  $\Gamma, \Delta \rightarrow \infty$ . A difficulty is that one has to show that also the derivatives are bounded in a similar manner, since we expect the relaxation solution  $x(t) \approx x_r(t)$  to give good approximations also concerning the slope of the periodic solution at the origin.

It is clear from (7.11) and (7.12) that an essential role is played by the solutions  $u_1(t)$ ,  $u_2(t)$  of the homogeneous linear equation:

$$\ddot{u}/\Gamma^{\frac{2}{3}} + (2\Delta) \dot{u}/\Gamma^{\frac{2}{3}} + 3y_r^2(t)u = 0 \quad (7.13)$$

For our purposes, it is enough to know asymptotic forms of these solutions (for large  $\Gamma, \Delta$ ): the change of variables (7.7) leads from (7.13) to

$$\ddot{w}/\Gamma^{\frac{2}{3}} + (3y_r^2 - \Delta/2\rho)w = 0, \quad (7.14)$$

which is equivalent to (7.8).

Equation (7.14) is of the Schrödinger type and may be compared with the equation of motion of an electron in a periodic potential:

$$-\frac{\hbar^2}{2m}\phi'' + V(x)\phi = E\phi, \quad (7.15)$$

where we have replaced  $w$  by  $-\phi$ ,  $t$  by  $x$ ,  $3y_1^2$  by  $-V$ ,  $\hbar^2/2m$  by  $1/\rho^{3/2}$ , and  $\Delta/2\rho$  by  $-E$ . If one compares the allowed and forbidden energy bands with the stability regions, one has to take into account the damping factor  $e^{-\Delta t}$  in the definition of  $w(t)$ , eq.(7.7).

Equation (7.14) can, for large  $\Gamma$ , be solved by means of the WKB method. If the points  $\Gamma, \Delta$  lie asymptotically above the line  $\Delta \approx \Gamma^{3/2}$ , then  $\Delta/\rho \rightarrow \infty$  and consequently the asymptotic solutions of (7.14) are exponential functions with real,  $t$ -dependent exponents. A more careful discussion shows that the inclusion of the factor  $e^{-\Delta t}$  leads to decaying exponentials. For this situation ( $\Delta \gg \Gamma^{3/2}$ ) we can show that indeed the corrections to  $y_1$  coming from the iteration of (7.10) are negligible for large  $\Gamma$  and  $\Delta$ . The details will be presented elsewhere.

If  $\Delta$  increases like  $\Gamma^{3/2}$  or less quickly, there are turning points of the WKB equation (7.14) that get close to each other as  $\Delta/\rho \rightarrow 0$ . Since  $y_1^2 \approx t^{3/2}$  near its zero, the distance  $d$  between the turning points is  $O[(\Delta/\rho)^{2/3}]$  and the wavelength  $\lambda$  is  $O[1/\Gamma^{3/2}/(\Delta/\rho)^{2/3}]$ . The condition of applicability of the WKB method is  $d \gg \lambda$ , which is in fact  $\Delta \gg \Gamma^{3/2}$ . Thus we again obtain the critical line of §7.1. The question of existence and uniqueness of the periodic solutions described above for large  $\Gamma$  and  $\Delta$  will be discussed and answered affirmatively in [8].

8. The limit  $\Gamma \rightarrow \infty$  and  $\Delta \ll \Gamma^{1/2}$

If the damping term increases less quickly than  $\Gamma^{1/2}$ , then the relaxation equation is no longer expected to give a good uniform asymptotic description of the Duffing equation, as we have seen in §7.1. Using scaling transformations, we noticed there that a boundary layer near  $t=0$  of order  $1/\Gamma^{1/2}$  appears instead, within which the equation of motion reads

$$\ddot{X} + X^3 = T, \quad \text{with } X = y\Gamma^{1/2}, \quad T = t\Gamma^{1/2}. \quad (8.1)$$

Here we assume a shift of the time scale by  $3\pi/2$ . In contrast to the relaxation equation, (8.1) does not admit of solutions which behave like  $T^{1/2}$  both for  $T \rightarrow \infty$  and for  $T \rightarrow -\infty$ . There does exist one solution that behaves like  $T^{1/2}$  as  $T \rightarrow -\infty$  and, using the symmetry  $T \rightarrow -T, X \rightarrow -X$  of (8.1), one solution that behaves like  $T^{1/2}$  as  $T \rightarrow +\infty$ . However, the two solutions are different from each other. The problem is then to decide on the boundary conditions that are used to pick out the relevant solution of (8.1). In general, it is not possible to decide on this and indeed, if for instance  $\Delta$  is a constant as  $\Gamma \rightarrow \infty$ , various solutions of (8.1) are relevant for the periodic asymptotic solution of Duffing's equation. However, if  $\Delta \rightarrow \infty$  as  $\Gamma \rightarrow \infty$ , then we expect that for  $t$  just before the boundary layer  $u(t) \approx 0$  and therefore  $y(t) \approx (\sin t)^{1/2}$  which is proportional to  $t^{1/2}$ . Thus it appears that in this domain of parameters, the boundary condition on (8.1) relevant for the periodic solution of Duffing's equation is  $X \approx T^{1/2}$  as  $T \rightarrow -\infty$ .

Clearly this particular solution of (8.1) may be obtained only numerically. The values of its slope at  $T=0$  and the value  $T_1$ , where it passes through zero, may be scaled back to obtain predictions for the slope  $\dot{x}(t=0)$ , the value  $x(t=0)$  and the position of the zero of the periodic solution  $x(t)$  of Duffing's equation, for large  $\Gamma$  and  $\Delta$  proportional to  $\Gamma^\alpha$  ( $\alpha < 1/2$ ):

$$\begin{aligned}
 x(3\pi/2) &= -0.67 \Gamma^{1/4} ; & \dot{x}(3\pi/2) &= 0.47 \Gamma^{1/2} ; \\
 t(x=0)-3\pi/2 &= 0.96/\Gamma^{1/4} ; & t_1(u=0)-3\pi/2 &= 1.79/\Gamma^{1/4} , \quad (8.2)
 \end{aligned}$$

where  $t_1$  is the first zero of  $x(t)$  after  $t=3\pi/2$ .

The remarkable feature of these results is their independence on the damping  $\Delta$ , as long as  $\Delta \ll \Gamma^{1/4}$  and  $\Delta \rightarrow \infty$ , as  $\Gamma \rightarrow \infty$ . In contrast, the values of the same quantities for  $\Delta \gg \Gamma^{1/4}$  do have a dependence on  $\Delta$ , through the quantity  $\rho = \Gamma^{1/4}/(2\Delta)$ .

We have made a numerical evaluation of the Duffing equation in order to test the predictions of (8.2). Table 8.1 shows the calculated values divided by the prediction at  $\Delta=2$ . It is seen that the ratio goes to 1 as predicted in the limit of large  $\Gamma$ .

$\Gamma$	$10^4$	$10^6$	$10^8$
$t_1(u=0)-3\pi/2$	1.18	1.06	1.00
$t(x=0)-3\pi/2$	1.22	1.08	1.02
$x(3\pi/2)$	1.10	1.04	1.02
$v(3\pi/2)$	0.88	0.96	1.00

Table 8.1: Test of the prediction (8.2). The numbers are the exact values divided by the prediction for the limit of large  $\Gamma$ . They belong to  $\Delta=2$ , whereas the predictions are made for increasing  $\Delta$ .

Up to now, we have investigated only the scaling properties of the periodic solution, assuming that  $\Delta \rightarrow \infty$  as  $\Gamma \rightarrow \infty$ . In analogy to §3, it is also of interest to obtain an asymptotic expression for this solution.

After having obtained preliminary results on this, our attention was called to recent papers by Byatt-Smith [5,6], who derived such an asymptotic expansion in the case  $\Delta=\text{const}$ , where the



boundary conditions on the solutions of (8.1) are not prescribed. Our presentation differs to some extent from that in [5,6].

When  $\sin t \approx 1$ , we expect the periodic solution to approach  $(\sin t)^{1/3}$ ; the corrections are obtained by formally iterating the Duffing equation:

$$(1/\Gamma^{1/3})\ddot{y} + (2\Delta/\Gamma^{1/3})\dot{y} + y^3 = \sin t ; \quad (8.3)$$

$$y_{\text{out};1}(t) = (\sin t)^{1/3} + (2/27) \frac{1}{\Gamma^{1/3}} \cos^2 t / (\sin t)^{2/3} \\ + \frac{1}{9\Gamma^{1/3}} \left[ 1/(\sin t)^{1/3} \right] - (2\Delta/\Gamma^{1/3}) \cos t / (\sin t)^{2/3} . \quad (8.4)$$

We now perform in (8.3) the change of variables:

$$t = T/\Gamma^{1/3} , \quad y = X/\Gamma^{1/6} \quad (8.5)$$

which turns it into:

$$\ddot{X} + 2\gamma\dot{X} + X^3 = \Gamma^{1/6} \sin (T/\Gamma^{1/3}) \approx T + T^3/6\Gamma^{1/3} + \dots \quad (8.6)$$

In (8.6),  $\gamma = \Delta/\Gamma^{1/3}$  and we have expanded the right hand side for  $T \ll \Gamma^{1/3}$ . As  $\Gamma \rightarrow \infty$ , we recognize that (8.6) goes over into the boundary layer equation (8.1). Consider now the solution  $X_0(T)$  of (8.1) which behaves like  $T^{1/3}$  as  $T \rightarrow +\infty$ . There exists just one such solution. It is not a solution of (8.6); there are corrections which may be obtained iteratively from (8.6):

$$X_{i;1}(T) = X_0(T) + \gamma X_1(T) + \dots \quad (8.7)$$

where  $X_1(T)$  is the solution that vanishes as  $T \rightarrow +\infty$  of the equation

$$\ddot{X}_1 + 3X_0^2(T)X_1 = -2\dot{X}_0 \quad (8.8)$$

etc. One verifies that the asymptotic expansion  $X_{i;1;as}(t)$  of (8.7) as  $T \rightarrow \infty$ , matches the expansion (8.4) as  $t \rightarrow 0$ , so that we expect

$$Y_0(t) = y_{out;1}(t) + (1/\Gamma^{1/2}) X_{i;1}(t\Gamma^{1/2}) - (1/\Gamma^{1/2}) X_{i;1;as}(t) \quad (8.9)$$

to be a uniform approximation to a solution of (8.3) on the whole interval  $[0, \pi/2]$ .

Our interest lies, however, in the solution  $X(T)$  of (8.1) which behaves like  $T^{1/3}$  as  $T \rightarrow \infty$  and this solution is different from  $X_0(T)$ . So we write

$$X(T) = X_0(T) + X_r(T) , \quad (8.10)$$

where  $X_r(T)$  verifies the equation

$$\ddot{X}_r + 3\dot{X}_r X_0^2(T) + 3X_r^2 \dot{X}_0(T) + X_r^3 = 0 . \quad (8.11)$$

Initial conditions for (8.11) are obtained from (8.10) and the definitions of  $X(T)$  and  $X_0(T)$ . The next problem is that of obtaining an asymptotic expansion of  $X_r(T)$ . This is not very easy. For  $T$  large,  $X_0(T) \approx T^{1/3}$  and the transformations  $\eta = T^{1/3}$ ,  $X_r(T) = P(\eta)/\eta^{1/3}$  change (8.11) into

$$d^2P/d\eta^2 + P(27/16 + 9/64\eta^2) + (27/16)P^2/\eta^{1/3} + (9/16)P^3/\eta^{1/3} = 0 . \quad (8.12)$$

Clearly, as  $\eta \rightarrow \infty$ , (8.12) tends to the equation of motion of a free oscillator with frequency  $\omega_0 = 3\sqrt{3}/4$ . However, it is only true that the energy  $E(\eta) = \omega_0^2 P^2/2 + (dP/d\eta)^2/2$  tends to a finite

limit as  $\eta \rightarrow \infty$ ; the phase does not behave like  $\omega_0 \eta + \text{const}$  for large  $\eta$ . The reason lies in the small power of  $1/\eta$  multiplying the nonlinear terms. The behavior of the phase may be obtained by going over to polar variables,  $R(\eta) = (2E(\eta))^{1/2}$ ,  $\tan \phi(\eta) = (dP/d\eta)/P(\eta)$  and applying Bogolyubov-Krylov averaging to the resulting equations. The equations satisfied by  $R(\eta)$ ,  $\phi(\eta)$  look complicated but they simplify considerably after averaging. In fact, one has to perform the average to the second order (i.e. in  $O(1/\eta^{3/4})$  and  $O(1/\eta^{5/4})$ ).

Averaging of the equation containing  $dR/d\eta$  leads to  $d\bar{R}/d\eta = 0$  both in  $O(1/\eta^{3/4})$  and  $O(1/\eta^{5/4})$ , i.e.  $R = \bar{R}_0 + O(1/\eta^{3/4})$ ; on the other hand, the equation for  $\phi(\eta)$  gives, after removing terms of  $O(1/\eta^{3/4})$  and averaging:

$$d\phi/d\eta = \omega_0 + (R^2/\eta^{3/4})(7\omega_0)/24 \quad (8.13)$$

so that

$$\phi(\eta) = \omega_0 \eta - (7\sqrt{3}/8)R_0^2 \eta^{1/4} + O(1) \quad (8.14)$$

Thus,

$$X_{r;as}(T) = (R_0/\eta^{1/4}) \cos \left[ \omega_0 \eta - (7\sqrt{3}/8)R_0^2 \eta^{1/4} + \phi_0 \right] + O(1/\eta^{3/4}). \quad (8.15)$$

The numbers  $R_0, \phi_0$  may be determined only by explicit integration of the differential equation (8.1) with the boundary condition  $X \rightarrow T^{1/4}$  as  $T \rightarrow \infty$ .

Clearly, outside the boundary layer  $t=O(\Gamma^{-1/4})$  the oscillations (8.15) decay due to damping, but this effect is not yet incorporated in the outer expansion (8.4). Taking (8.5) into account, we see that the corrections to the solution  $y(t)$ , due to (8.15) are:

$$0\left[1/(\Gamma^{1/2}\eta^{1/2})\right] = 0\left[1/(\Gamma^{1/2}\tau^{1/2})\right] = 0\left[1/(\Gamma^{1/2}\Gamma^{1/2})\right] = 0\left[1/(\Gamma^{1/2})\right] . \quad (8.16)$$

Thus, we look for solutions of (8.3), for  $t \gg 1/\Gamma^{1/2}$  in the form of an expansion:

$$y(t) = y_{\text{out};1}(t) + (1/\Gamma^{1/2})u_1(t) + (1/\Gamma^{1/2})u_2(t) + \dots \quad (8.17)$$

This is the analogon of equations (3.18-19) of [6]. We substitute (8.17) into (8.3) and equate coefficients of like powers of  $(1/\Gamma^{1/2})$  (up to  $1/\Gamma^{1/2}, \Delta/\Gamma^{1/2}$ ). This gives to first orders:

$$(1/\Gamma^{1/2})\ddot{u}_1(t) + (2\Delta/\Gamma^{1/2})\dot{u}_1(t) + 3y_{\text{out};1}^2(t)u_1(t) = 0 , \quad (8.18a)$$

$$(1/\Gamma^{1/2})\ddot{u}_2(t) + (2\Delta/\Gamma^{1/2})\dot{u}_2(t) + 3y_{\text{out};1}^2(t)u_2(t) = -3u_1(t)u_2(t) . \quad (8.18b)$$

Equation (8.18a) describes a decaying oscillation, which may be treated in an adiabatic approximation if one uses the time  $\tau = \Gamma^{1/2}t$ . One obtains the ansatz equation (7.9) for the solution. The constant  $U_0$  and the phase are fixed from the condition that as  $t \rightarrow 0$ , we should obtain (8.15). However, there is clearly a difficulty: the term of the phase containing  $\eta^{1/2}$ , i.e.  $\tau^{1/2}$ , cannot yet be reproduced. This correction is proportional to  $\Gamma^{1/2}$ .

The reason lies in the fact that in the analogon of (8.18b) written for  $u_2(t)$  there appear resonant terms on the right hand side (with respect to the fast variable  $\tau$ ), so that there are no periodic solutions. Thus one has to apply the method of Lindstedt and Poincaré and allow for the addition to the frequency  $y_{\text{out};1}(\tau/\Gamma^{1/2})$  of a power series in  $1/\Gamma^{1/2}$  with coefficients functions of  $\tau/\Gamma^{1/2}$ . Since there are no secular terms in the equation of  $u_2(t)$ , the first term in the series is  $O(1/\Gamma^{1/2})$ . Returning to the original time variable, i.e. writing in the phase the factor  $\Gamma^{1/2}$  explicitly, we obtain a correction of  $O(\Gamma^{1/2})$  as desired.

With this, we expect the asymptotic expansion for the periodic solution in the interval  $[0, \pi/2]$  to be:

$$y(t) = Y_0(t) + (1/\Gamma^{1/2})x_r(t\Gamma^{1/2}) - (1/\Gamma^{1/2})x_{r;as}(t\Gamma^{1/2}) \\ + (1/\Gamma^{1/2})u_1(t) + (1/\Gamma^{1/2})u_2(t) + \dots \quad (8.19)$$

A periodic solution is obtained by subtracting  $y_{out;1}(t)$  from (8.19), repeating the result periodically with appropriate sign changes and then adding  $y_{out;1}(t)$ .

### 9. The Fourier expansion of $x(t)$ at large $\Gamma$

We show in Fig.9.1 the ratios  $c_n/c_1$  of the Fourier coefficients of the expansion

$$x(t) = \sum c_n \cos(nt - \chi_n) \quad (9.1)$$

for a harmonic solution at  $\Gamma=1000$ ,  $\Delta=1$ , which has nonvanishing coefficients only for odd values of  $n$ . The result is compared with the coefficients of the expansions for  $x_r(t)$  and for  $x_{\infty}(t)$ .

It is seen that the ratios agree very well up to  $n=5$ . Then, the coefficients of  $x(t)$  tend towards a peak at  $n=15$ , which belongs to the rapid oscillations of  $u(t)$ . The convergence is slower for  $x_{\infty}(t)$  than in the other cases because the derivative becomes infinite at the zeros of this function.

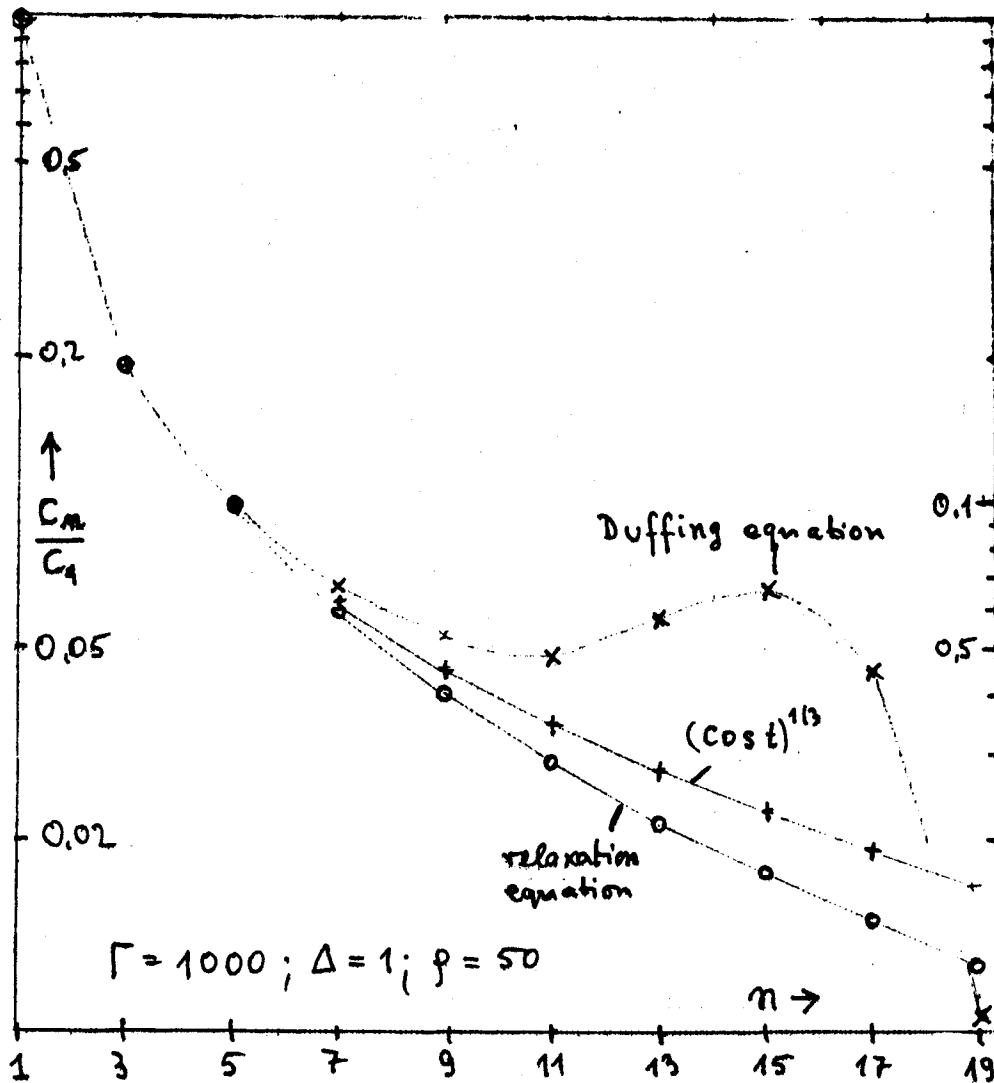


Fig.9.1: Ratios of the Fourier coefficients  $c_n/c_1$  for  $x(t)$ ,  $x_r(t)$  and  $x_\infty(t)$  at  $\Gamma=1000$ ,  $\Delta=1$ .

From numerical evaluations of the Duffing equation, one obtains with  $\Delta$  in a wide range (0.1...50) and large  $\Gamma$  the result  $c_1/\Gamma^{1/2} \approx 1.16$ . It is remarkable that the first order of the method of harmonic balance gives  $c_1/\Gamma^{1/2} = 1.1006$  and the second order 1.145, i.e. the results for  $c_1$  are almost correct although the solutions  $x(t)$  are much different from each other [2]. The second-order method gives in addition for large  $\Gamma$  the ratio  $c_1/c_3 = 0.165$ , which differs by only 20% from the value obtained from the numerical solution of the Duffing equation.

## 10. Summary

We have investigated the behavior of the harmonic solutions of the Duffing equation

$$\ddot{x} + 2\Delta\dot{x} + x^3 = \Gamma \cos t \quad (10.1)$$

for large values of the parameters  $\Gamma$  and various values of  $\Delta$ . First, we recall our conclusions in the case that  $\Gamma \rightarrow \infty$  and  $\Delta$  increases as  $\Gamma^\alpha$ . All statements remain valid if a linear term  $kx$  is added on the left hand side of (10.1) and  $k$  is kept constant. As  $\Gamma \rightarrow \infty$ , this term never contributes to the leading asymptotic approximation of the solution.

### 10.1 The leading term in $x(t)$ for $\Gamma \rightarrow \infty$ , $\Delta = \text{const} \cdot \Gamma^\alpha$

$\alpha > \frac{2}{3}$ :

$x(t) \approx (\Gamma/2\Delta) \sin t$ ;  $\rho = \Gamma^{2/3}/2\Delta \rightarrow 0$ ;  $\ddot{x}$  and  $x^3$  are negligible.

$\alpha = \frac{2}{3}$ :

$x(t) \approx x_r(t)$ , where  $x_r$  is the periodic solution of

$$2\Delta x_r + x_r^3 = \Gamma \cos t, \quad (10.2)$$

$\rho = \text{const}$ ,  $\ddot{x}$  is negligible.

$\frac{2}{3} > \alpha > \frac{1}{3}$ :

$x(t) \approx x_r(t)$ ;  $x_r(t) \approx x_\infty(t) \approx (\Gamma \cos t)^{1/3}$  if  $|t - \pi/2 - N\pi| > 1/\rho^{3/2}$ .

As  $\Gamma \rightarrow \infty$ ,  $\rho \rightarrow \infty$ , and  $\ddot{x}$  and  $2\Delta\dot{x}$  are negligible.

$\frac{1}{2} > \alpha > 0$ :

$x(t) \approx x_r(t)$  if  $|t - \pi/2 - N\pi| > 1/4$ , see (8.19).

$\alpha = 0$ :

$$x(t) = X_\infty(t) + O(1/\Gamma^{\frac{1}{2}})$$

10.2 The magnitude of  $u(t) = x(t) - x_r(t)$  as  $\Gamma \rightarrow \infty$ ,  $\Delta = \text{const} \cdot \Gamma^\alpha$

$\frac{1}{2} > \alpha > \frac{1}{4}$ :

Within the boundary layer  $u(t)$  has a dip-bump structure which vanishes as  $\Gamma$  increases. It is of order  $1/\rho$  elsewhere.

$\alpha = \frac{1}{4}$ :

The exponent of the damping factor  $e^{-\Delta t}$  for one  $u$ -oscillation  $(2\pi/\omega_u)\Delta$  is of order 1.

$\frac{1}{2} > \alpha > \frac{1}{4}$ :

$u(t)$  may have oscillations within the boundary layer.

$\alpha = \frac{1}{4}$ :

$\Delta$ -width of the boundary layer is of order 1.

$\frac{1}{2} > \alpha > 0$ :

At large finite values of  $\Gamma$ , the above mentioned dip-bump structure of  $u(t)$  in the boundary layer is continued in the form of oscillations, which are damped as  $e^{-\Delta t}$  for  $t > 1/\Gamma^{\frac{1}{2}}$ . For sufficiently large values of  $\Gamma$ ,  $u(t) \approx 0$  at the beginning of the next boundary layer.



$\alpha = 0, \Delta = \text{const:}$

If  $\pi\Delta \ll 1$ ,  $u(t)$  arrives at the left hand sides of the boundary layers with a relatively large amplitude. As  $\Gamma \rightarrow \infty$ , the maximum of  $|u/x_r|$  goes to zero as  $1/\Gamma^{1/2}$ , i.e. very slowly.

### 10.3 Widths of the boundary layers

$\frac{1}{2} > \alpha > \frac{1}{4}$ : Width =  $O(1/\rho^{1/2})$ .

$\frac{1}{2} > \alpha > 0$ : Width of the inner boundary layer =  $O(1/\Gamma^{1/4})$ .

### 10.4 Approximations for $x(t)$ and $u(t)$ outside the boundary layers

For large  $\Gamma$ ,  $x(t) \approx x_{\infty}(t)$ . If  $|u/x_r|$  is small,  $u(t)$  has been calculated from the adiabatic approximation for the motion in a slowly time-dependent parabolic potential. If the ratio is larger, the anharmonic terms of the potential lead to an asymmetric oscillation of  $u(t)$ . A quasistatic approximation gives good results. The adiabatic approximation should be even better, but it has not yet been calculated for this case.

### 10.5 Calculations for finite values of $\Gamma$ and $\Delta$

In addition to the treatment of various limits  $\Gamma \rightarrow \infty$ , we have studied in large domains of the  $\Gamma, \Delta$ -plane approximations based on the decomposition  $x(t) = x_r(t) + u(t)$ , where  $x_r(t)$  fulfills the relaxation equation (10.2). This decomposition is related to the physical description as the motion of a particle in a slowly time-dependent potential. From the equation for  $u(t)$ , which is equivalent to the Duffing equation, one can guess approximations which are much less obvious if one works with (10.1).

### Acknowledgments

We are grateful to W. Lauterborn for calling our attention to the recent papers by J.G. Byatt-Smith.

### References

- [1] Hayashi, C.: Nonlinear Oscillations in Physical Systems (McGraw Hill 1964).
- [2] Höhler, G.: Schwingungen II, to appear in "Computer Theoretikum and Praktikum für Physiker" No.3 (Fachinformationszentrum Karlsruhe, 7514 Eggenstein-Leopoldshafen 2, 1988). This series of lecture notes is a guide to the application of personal computers in theoretical physics.
- [3] Bender, C.M. and Orszag, St.: Advanced Mathematical Methods for Scientists and Engineers (McGraw Hill 1978).
- [4] Parlitz, U. and Lauterborn, W: Z. Naturforsch. 41a, 605 (1986); Parlitz, U.: Thesis, University of Göttingen 1987.
- [5] Byatt-Smith, J.G.: IMA J. Appl.Math. 37, 113 (1986).
- [6] Byatt-Smith, J.G.: SIAM 47, 1 (1987).
- [7] Lichtenberg, A.J. and Liebermann, M.A.: Regular and Stochastic Motion (Springer 1983), §2.3.
- [8] Sabba-Stefanescu, I.: to be published.